Journal of Oceanography, Vol. 56, pp. 591 to 599, 2000

Short Contribution

P-Vector Spirals and Determination of Absolute Velocities

PETER C. CHU*

Naval Postgraduate School, Monterey, CA 93943, U.S.A.

(Received 26 July 1999; in revised form 14 December 1999; accepted 18 February 2000)

A simple method to invert the absolute geostrophic velocity on potential-density surfaces is developed based on McDougall's (1988) conservation statements on potential-density surfaces and Chu's (1995) and McDougall's (1995) P-vector concept. This method has a capability to handle a system with diapycnal velocities and non-coincidence of potential-density and neutral surfaces. The validity of the inversion is the existence of the P-vector spirals instead of the existence of the velocity spirals (usually called the β-spirals). We use a climatological *T, S* dataset for the Atlantic Ocean from the National Oceanographic Data Center (NODC) to show the benefit of using P-vector spirals in inverting the velocity field.

Keywords:
· P-vector spiral,
· absolute velocity,
· potential density surface,
· diapycnal velocity,
· inverse method.

1. Introduction

Our understanding of the mid-latitude large-scale ocean circulation has been benefitted by a set of papers by Stommel and collaborators (Stommel and Schott, 1977; Schott and Stommel, 1978; Behringer and Stommel, 1980), Wunsch and collaborators (Wunsch, 1978; Wunsch and Grant, 1982), Killworth (1986), and Chu and collaborators (Chu, 1995; Chu *et al*., 1998a, b). Their work makes it possible to obtain ocean general circulations from observations of temperature (T) and salinity (S). The physical base for calculating geostrophic velocity from hydrographic data is the thermal wind relation

$$\boldsymbol{V} = \boldsymbol{V}_0 + \frac{1}{f}\boldsymbol{k}\times\int_{z_0}^{z}\nabla\left[\frac{\partial}{\partial z}\left(\frac{p}{\rho}\right)\right]dz', \tag{1}$$

where (x, y, z) are the three axes with corresponding unit vectors $(\boldsymbol{i}, \boldsymbol{j}, \boldsymbol{k})$ of the Cartesian coordinates pointing eastward, northward, and upward, respectively; $\nabla = \boldsymbol{i}\partial/\partial x + \boldsymbol{j}\partial/\partial y$, is the two dimensional gradient operator; $\boldsymbol{V} = (u, v)$, $\boldsymbol{V}_0 = (u_0, v_0)$ are the geostrophic velocities at any depth z and at a reference depth z_0, p is the pressure, g is the gravitational acceleration, and f is the Coriolis parameter, which is a function of latitude. As mentioned by Olbers *et al*. (1985), the quantities T, S are relatively easy to measure, and in contrast to velocity observations, the climatological signal in the T, S fields is less contaminated by energetic smaller-scale motions induced by eddies and waves. Usually, the hydrographic data only determine the relative geostrophic currents with the Boussinesq approximation,

$$\boldsymbol{V}' = \frac{1}{f}\boldsymbol{k}\times\int_{z_0}^{z}\nabla\left[\frac{\partial}{\partial z}\left(\frac{p}{\rho}\right)\right]dz' = -\frac{g}{f\rho_0}\boldsymbol{k}\times\int_{z_0}^{z}\nabla\rho dz'. \tag{2}$$

The reference velocity $\boldsymbol{V}_0$ still needs to be determined.

Davis (1978) pointed out that the β-spiral method (Stommel and Schott, 1977) and the box method (Wunsch, 1978), no matter how different in appearance, are based on the same order of dynamical sophistication and differ from implicit assumptions about the scales of oceanic variability and different definitions of the smooth field to which the dynamical model pertains. The physical principle for both methods are the existence of a conservative tracer which allows determination of a family of material (usually the potential vorticity) surfaces $z = h(x, y)$ such that

$$\nabla\bullet\int_{h_n}^{h_{n+1}} dz\left[\boldsymbol{V}' + \boldsymbol{V}_0\right] = 0. \tag{3}$$

For steady flow in an ideal and incompressible ocean, density (ρ), and potential vorticity (q) are materially conserved.

Shortly after the β-spiral method was proposed, Schott and Stommel (1978) reported that in some in-

* E-mail address: pcchu@nps.navy.mil

stances the absolute velocity computed at a constant reference level depends on the depth range of data used in the computation. Behringer (1979) thought that this ambiguity was caused by large error in calculating ϕ in the z-level. Here, ϕ is the angle between the horizontal absolute velocity vector and the eastward direction. He proposed a two-step procedure to reduce this ambiguity: (a) determination of ϕ on isopycnal surfaces, and (b) determination of the reference velocities. Taking the variation of (3) with respect to h to obtain (Davis, 1978)

$$\boldsymbol{V}_0 \cdot \nabla \partial_z h - \frac{\beta}{f} v_0 = -\partial_z (\boldsymbol{V}' \cdot \nabla h) \frac{\beta}{f} v' \qquad (4)$$

which differs from the original β-spiral method (Stommel and Schott, 1977) by the term $\nabla h \cdot [\partial_z' \boldsymbol{V}]$. Coats (1981) used (4) to calculate the absolute velocity in the northeastern Pacific Ocean.

Keeping the dynamical system as geostrophic and hydrostatic balanced and adding diapycnic and isopycnic turbulent mixing terms in the tracer equations (i.e., heat, salt, and potential vorticity equations), Olbers *et al*. (1985) applied the β-spiral technique to the climatological hydrographic atlas of the North Atlantic Ocean and obtained the velocity field resemblance of the classical view of the North Atlantic circulation.

The intersections of isopycnals with surfaces of constant q must parallel to streamlines, and thus the direction of velocity is one of the two opposite directions (180° apart) at each level. Behringer (1979) appears to be the first to employ potential density and potential vorticity to determine flow direction but did not combine results from different levels to establish velocity (Davis, 1978). When considering the absolute horizontal velocity at two levels, the magnitudes can be determined by the thermal wind relation. Apparently, the method fails if isopycnals and surfaces of constant potential vorticity coincide so that the velocity direction cannot be determined (necessary condition 1). Another case of failure arrises when the absolute horizontal velocity vector does not turn with depth (necessary condition 2) and so incompatibility with the relative velocity profiles can occur (Olbers *et al*., 1985). The two necessary conditions for the validity of the β-spiral method can be easily identified by a unit vector

$$\boldsymbol{P} = \frac{\nabla\rho \times \nabla q}{|\nabla\rho \times \nabla q|}$$

which is determined by the density field only (Chu, 1995; Chu *et al*., 1998a, b). Existence of this unit vector ($\boldsymbol{P}$) implies the satisfaction of necessary condition 1. Existence of the vertical turning of $\boldsymbol{P}$ indicates the satisfaction of necessary condition 2. Inversion of the absolute velocity ($\boldsymbol{V} = \gamma \boldsymbol{P}$) is divided into two steps: (a) determination of the vector $\boldsymbol{P}$, and (b) determination of γ.

McDougall (1988) developed a consistent formulation for the β-spiral in an isopycnal framework. Later on, he obtained the absolute horizonal velocity on the neutral surface from vertical differentiation of the potential vorticity equation with the thermal wind relation (McDougall, 1995). Following McDougall's (1988, 1995) framework, we develop a simple method to invert the absolute velocity on isopycnal surfaces from hydrographic data.

The outline of this paper is as follows. We introduce McDougall's (1988) conservation statements on potential-density surfaces in Section 2, and present concepts of the P-vector on the potential-density surface, two necessary conditions for the inversion, and the P-vector spiral in Sections 3–5. In Section 6, we establish climatological annual mean isopycnal depth, potential vorticity, and $\boldsymbol{P}$-spiral parameter data sets for the Atlantic Ocean from a climatological T, S data produced by the National Oceanographic Data Center (NODC) (Levitus and Boyer, 1994; Levitus *et al*., 1994). In Section 7, we investigate the inverted latitudinal volume transport. In Section 8 we present our conclusions.

2. Conservation Statements on Potential-Density Surfaces

Consider a series of potential density (σ_θ) surfaces, each marked by a constant value of σ, and with the depth

$$z^{(\sigma)} = R(x, y, \sigma).$$

The vertical distance between two closely-spaced σ surfaces with increment of $\Delta\sigma$ is given by

$$h^{(\sigma)} = \frac{\partial z^{(\sigma)}}{\partial \sigma} \Delta\sigma. \qquad (5)$$

The conservation on the potential-density surface is given by McDougall (1988)

$$\boldsymbol{V}^{(\sigma)} \cdot \nabla_\sigma \left[q^{(\sigma)} \right] = \frac{\partial w^{(\sigma)}}{\partial z}, \quad q^{(\sigma)} = \ln\left[Q^{(\sigma)} \right], \quad Q^{(\sigma)} = \frac{f}{h^{(\sigma)}} \qquad (6)$$

where $\boldsymbol{V}^{(\sigma)}$ and ∇_σ are the lateral velocity and gradient operator (two-dimensional) along the potential density surface; $Q^{(\sigma)}$ is the potential vorticity; $q^{(\sigma)}$ is a conservative quantity representing the potential vorticity (we may call it the pseudo potential vorticity), and $w^{(\sigma)}$ is the diapycnal velocity through a σ-surface. The diapycnal velocity $w^{(\sigma)}$ has contributions not only from the vertical diffusivity, thermobaricity and cabbeling, but also from

lateral mixing along the neutral tangent plane (McDougall, 1988).

McDougall (1988) further derived the following thermal wind relation for the potential density surfaces,

$$\frac{\partial \boldsymbol{V}^{(\sigma)}}{\partial z} = \frac{N^2}{f}\boldsymbol{k}\times\nabla_\sigma\left(\frac{p}{g\rho}\right) + \boldsymbol{k}\times\left[\frac{1-1/\mu}{\theta_z}\right]\nabla_\sigma\theta \quad (7)$$

where N is the buoyancy frequency; θ is the potential temperature, and μ is the factor indicating the difference between the potential-density and neutral surfaces. The neutral surface is defined as a surface along which fluid parcels can be moved a small distance without experiencing a gravitational restoring force. If μ = 1, the neutral surface coincides with the potential-density surface (McDougall, 1988). In this paper, we call the case of μ = 1 as the no μ-effect case (no difference between the neutral surface coincides with the potential-density surface) and the case of $\mu \neq 1$ as the μ-effect case (difference between the neutral surface coincides with the potential-density surface).

3. P-Vector on Potential-Density Surface

Following Chu (1995), we may define two orthogonal vectors on the potential density surface

$$\boldsymbol{P} = \frac{1}{\left|\nabla q^{(\sigma)}\right|}\left(\frac{\partial q^{(\sigma)}}{\partial y}\boldsymbol{i} - \frac{\partial q^{(\sigma)}}{\partial x}\boldsymbol{j}\right), \quad \boldsymbol{N} = \frac{\nabla_\sigma\left(q^{(\sigma)}\right)}{\left|\nabla_\sigma\left(q^{(\sigma)}\right)\right|} \quad (8)$$

which are the tangential and normal unit vectors of the q_σ-isolines (Fig. 1). Using (8), the velocity vector $\boldsymbol{V}_\sigma$ can be decomposed as

$$\boldsymbol{V}^{(\sigma)} = \gamma\boldsymbol{P} + \frac{\partial w^{(\sigma)}/\partial z}{\left|\nabla_\sigma\left(q^{(\sigma)}\right)\right|}\boldsymbol{N} \quad (9)$$

which is similar to McDougall's (1995) formulation. Here, γ is the parameter to be determined by the thermal wind relation (7). Vertically varying diapycnal velocity ($\partial w^{(\sigma)}/\partial z \neq 0$) causes the crossing $q^{(\sigma)}$-isoline motion.

Use of (6) leads to

$$P_x = \left(\frac{\beta}{f} - \frac{\partial \ln h^{(\sigma)}}{\partial y}\right)\Bigg/\left[\left(\frac{\beta}{f} - \frac{\partial \ln h^{(\sigma)}}{\partial y}\right)^2 + \left(\frac{\partial \ln h^{(\sigma)}}{\partial x}\right)^2\right]^{1/2} \quad (10)$$

$$P_y = \frac{\partial \ln h^{(\sigma)}}{\partial x}\Bigg/\left[\left(\frac{\beta}{f} - \frac{\partial \ln h^{(\sigma)}}{\partial y}\right)^2 + \left(\frac{\partial \ln h^{(\sigma)}}{\partial x}\right)^2\right]^{1/2}$$

where P_x and P_y are the components of the vector $\boldsymbol{P}$.

Without vertical change of the diapycnal velocity equation (9) becomes,

$$\boldsymbol{V}^{(\sigma)} = \gamma\boldsymbol{P} \quad (11)$$

and any water particle moves along $q^{(\sigma)}$-isolines on the potential density, i.e., any $q^{(\sigma)}$-isoline is a trajectory of water particles (Fig. 1). We call this case ($\partial w^{(\sigma)}/\partial z \neq 0$) as the no diapycnal exchange case.

4. Necessary Conditions for Inversion

Applying the thermal wind relation (7) to any two different potential density levels σ_k and σ_m (the corresponding depths z_k and z_m), shown as in Fig. 2(a), a set of algebraic equations for determining the parameter γ is obtained

$$\begin{aligned}\gamma^{(k)}P_x{}^{(k)} - \gamma^{(m)}P_x{}^{(m)} &= \Delta u_{km} = \Delta^{(0)}u_{km} + \Delta^{(\mu)}u_{km} + \Delta^{(w)}u_{km}\\ \gamma^{(k)}P_y{}^{(k)} - \gamma^{(m)}P_y{}^{(m)} &= \Delta v_{km} = \Delta^{(0)}v_{km} + \Delta^{(\mu)}v_{km} + \Delta^{(w)}v_{km}\end{aligned} \quad (12)$$

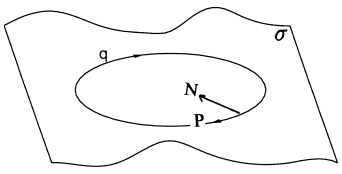

Fig. 1. Isoline of potential vorticity (q) is the trajectory on the isopycnal surface.

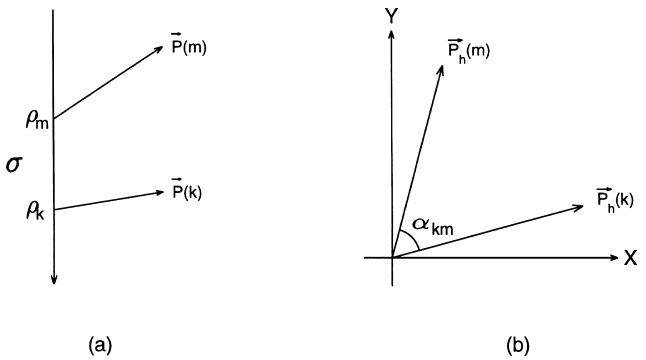

Fig. 2. Vertical turning of the P-vector: (a) P vector at two isopycnal levels, and (b) turning angle between two isopycnal levels.

which are two linear algebraic equations for $\gamma^{(k)}$ and $\gamma^{(m)}$. Here $\gamma^{(i)} = \gamma(x, y, \sigma_j)$, and

$$\left(\Delta^{(0)}u_{km}, \Delta^{(0)}v_{km}\right) = \int_{z_m}^{z_k} \frac{N^2}{f}\boldsymbol{k}\times\nabla_\sigma\left(\frac{p}{g\rho}\right)dz \qquad (13)$$

is the vertical shear of $\boldsymbol{V}^{(\sigma)}$ with no μ-effect and no diapycnal velocity. With the μ-effect and diapycnal velocity, we will have two extra source terms ($\Delta^{(\mu)}u_{km}$, $\Delta^{(\mu)}v_{km}$) and ($\Delta^{(w)}u_{km}$, $\Delta^{(w)}v_{km}$) on the right-hand sides of (12). As soon as $\gamma^{(k)}$ is obtained, the velocity field can be computed by (9) or (11).

If the determinant

$$\begin{vmatrix} P_x^{(k)} & P_x^{(m)} \\ P_y^{(k)} & P_y^{(m)} \end{vmatrix} \neq 0$$

the algebraic equations (12) have definite solutions for $\gamma^{(k)}$ ($m \neq k$):

$$\gamma^{(k)} = \frac{\begin{vmatrix} \Delta u_{km} & P_x^{(m)} \\ \Delta v_{km} & P_y^{(m)} \end{vmatrix}}{\begin{vmatrix} P_x^{(k)} & P_x^{(m)} \\ P_y^{(k)} & P_y^{(m)} \end{vmatrix}}. \qquad (14)$$

The determinant in the denominator of (14) is the sine of the vertical turning angle between $\boldsymbol{P}^{(k)}$ and $\boldsymbol{P}^{(m)}$ (Fig. 2(b)). The solution exists if

$$\begin{vmatrix} P_x^{(k)} & P_x^{(m)} \\ P_y^{(k)} & P_y^{(m)} \end{vmatrix} \equiv \sin\left(\phi_{km}\right) \neq 0 \qquad (15)$$

where ϕ_{km} indicates the P-vector turning angle between the two levels σ_k and σ_m.

The conventional view on the validity of the inversion is the existence of velocity spiral, which is called the β-spiral by Stommel and Schott (1977). This is true only for a system with no μ-effect and no diapycnal velocity. For a system with either the μ-effect or the diapycnal velocity, the validity of the inversion is no longer the existence of velocity spiral, but the existence of the P-vector spiral ($\phi_{km} \neq 0$). Therefore, we have the benefit of use of the unit vector, $\boldsymbol{P}$, because the existence of $\boldsymbol{P}$ is equivalent to the intersection of isopycnals and surfaces of constant potential vorticity (necessary condition 1); and the existence of the $\boldsymbol{P}$-spiral is required for the inversion (necessary condition 2).

5. P-Vector Spiral

McDougall (1995) first presented the $\boldsymbol{P}$-spiral concept on the neutral surface. Letting ϕ be the angle measured counterclockwise from the x-axis to the vector $\boldsymbol{P}$ (McDougall, 1995), we have

$$\cos\phi = P_x, \quad \sin\phi = P_y. \qquad (16)$$

Existence of the $\boldsymbol{P}$-spiral between potential-density levels becomes the nonzero $\partial\phi/\partial z^{(\sigma)}$. We may define a nondimensional parameter (i.e., the $\boldsymbol{P}$-spiral parameter)

$$\Lambda = h^{(\sigma)}\frac{\partial\phi}{\partial z^{(\sigma)}} \qquad (17)$$

to describe the $\boldsymbol{P}$-spiral. Substitution of (16) into (17) leads to

$$\Lambda = -h^{(\sigma)}\frac{\partial P_x / \partial z^{(\sigma)}}{P_y} = h^{(\sigma)}\frac{\partial P_y / \partial z^{(\sigma)}}{P_x} \qquad (18)$$

and substitution of (10) into (18) leads to

$$\Lambda = h^{(\sigma)}\frac{J\left(q^{(\sigma)}, \partial q^{(\sigma)} / \partial z^{(\sigma)}\right)}{\left|\nabla_\sigma\left(q^{(\sigma)}\right)\right|^2} \qquad (19)$$

where

$$J(A, B) \equiv \frac{\partial A}{\partial x}\frac{\partial B}{\partial y} - \frac{\partial B}{\partial x}\frac{\partial A}{\partial y}$$

is the Jacobian.

Thus, the necessary condition for occurrence of the $\boldsymbol{P}$-spiral is the non-zero Jacobian of $q^{(\sigma)}$ and $\partial q^{(\sigma)}/\partial z^{(\sigma)}$, that is, the nonzero $q^{(\sigma)}$ and $\partial q^{(\sigma)}/\partial z^{(\sigma)}$, and the independence between $q^{(\sigma)}$ and $\partial q^{(\sigma)}/\partial z^{(\sigma)}$.

Substitution of (6) into (19) leads to

$$\Lambda = h^{(\sigma)}\frac{-\frac{\beta}{f}\frac{\partial^2\left[\ln h^{(\sigma)}\right]}{\partial x\partial z^{(\sigma)}} + J\left[\ln h^{(\sigma)}, \frac{\partial\left(\ln h^{(\sigma)}\right)}{\partial z^{(\sigma)}}\right]}{\left[\frac{\partial\left(\ln h^{(\sigma)}\right)}{\partial x}\right]^2 + \left[\frac{\beta}{f} - \frac{\partial\left(\ln h^{(\sigma)}\right)}{\partial y}\right]^2} \qquad (20)$$

which indicates that the ***P***-spiral can be generated by laterally and vertically inhomogeneous thickness between two closely-spaced potential-density surfaces. Recently, Chu and Li (2000) obtained the South China Sea isopycnal surface circulation using the P-vector sprial method.

6. Climatological Annual Mean $Z^{(\sigma)}$, $Q^{(\sigma)}$, and Λ Data

6.1 Division of potential density layers

We use three reference levels for the potential density computation: σ_0 for the surface, σ_2 for 2 km depth, and σ_4 for 4 km depth. Here,

$$\sigma_m = \rho - 1000 \text{ kg/m}^3, \quad m = 0, 2, 4. \tag{21}$$

The potential density σ_0, σ_2, and σ_4 represent upper, intermediate, and deep layers, respectively. We consider the following ranges for the σ_m-values:

$$25.01 \le \sigma_0 \le 27.99, \quad 33.11 \le \sigma_2 \le 37.09,$$
$$41.51 \le \sigma_4 \le 45.99. \tag{22}$$

Notice that the values of 28.00, 37.10, 46.0 are maximum values for σ_0, σ_2, and σ_4 computed from the NODC *T, S* data set. We further discretize σ_0, σ_2, and σ_4 with the same increment,

$$\Delta\sigma = 0.02 \text{ kg/m}^3. \tag{23}$$

Thus, we have 150 σ_0-layers, 200 σ_2-layers, and 225 σ_4-layers. Within each layer, the density is vertically uniform.

6.2 Establishment of hydrographic data with high vertical resolution

We use the NODC climatological *T, S* data for the Atlantic Ocean in this study. The data set has $1^\circ \times 1^\circ$ horizontal resolution and 33 vertical levels (Levitus and Boyer, 1994; Levitus *et al*., 1994). In order to well resolve potential-density surfaces, we use cubic spline to interpolate the *T, S* data into 236 *z*-levels with three different increments: 10 m from 0 to 1000 m depths, 20 m from 1000 to 2500 m depths, and 50 m from 2500 to 5500 m depths. Thus, we build up a high resolution *z*-coordinate data set $[\hat{T}(z_j),\ \hat{S}(z_j),\ \hat{\sigma}_0(z_j),\ \hat{\sigma}_2(z_j),\ \hat{\sigma}_4(z_j)]$. The symbol "^" indicates either the observational data or the values computed from the observational data.

6.3 Transformation of T, S data from z-coordinates to potential density surfaces

The transformation is fulfilled by comparing the *z*-coordinate potential density data $\hat{\sigma}(z_j) \equiv [\hat{\sigma}_0(z_j),\ \hat{\sigma}_2(z_j),\ \hat{\sigma}_4(z_j)]$, with the discrete σ-values, $\sigma(k)$. The two values refer to different dimensions: $\hat{\sigma}(z_j)$ for the depth $-z_j$, and $\sigma(k)$. Thus, we use the sigma value at the bottom of the *k*-th isopycnal layer, $\sigma^b(k)$, for the comparison,

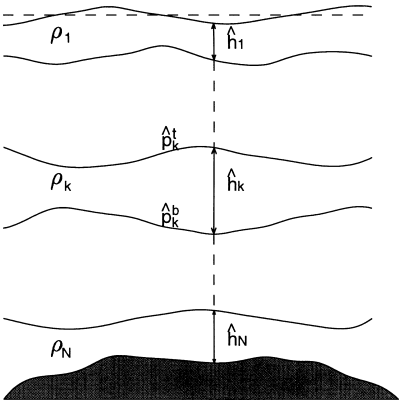

Fig. 3. Vertical discretization of the multi-layer ocean with the *k*-th layer having potential density ρ_k, layer thickness $\hat{h}_k$, top and bottom pressures ($\hat{p}_k{}^t$, $\hat{p}_k{}^b$), respectively.

$$\sigma^b(k) = \frac{1}{2}\left[\sigma(k) + \sigma(k+1)\right]. \tag{24}$$

The depth for the bottom of the $\sigma(k)$-layer is obtained by

$$\hat{z}_k^{(\sigma)} = z_j, \quad \text{if} \quad \hat{\sigma}\left(z_j\right) = \sigma^b(k) \tag{25}$$

and

$$\hat{z}_k^{(\sigma)} = z_j + \frac{\sigma(k) - \hat{\sigma}\left(z_j\right)}{\hat{\sigma}\left(z_{j+1}\right) - \hat{\sigma}\left(z_j\right)}\left(z_{j+1} - z_j\right),$$
$$\text{if} \quad \hat{\sigma}\left(z_j\right) < \sigma^b(k) < \hat{\sigma}\left(z_{j+1}\right) \tag{26}$$

where the superscript *b* indicates the bottom of the *k*-th isopycnal layer. The thickness of the *k*-th isopycnal layer is obtained by (Fig. 3)

$$\hat{h}_k^{(\sigma)} = \hat{z}_{k-1}^b - \hat{z}_k^b.$$

For the *k*-th potential-density layer $\sigma(k)$, the potential vorticity $\hat{Q}_k{}^{(\sigma)}$ and the pseudo potential vorticity $q_k{}^{(\sigma)}$ are computed by

$$\hat{Q}_k^{(\sigma)} = \frac{f}{\hat{h}_k^{(\sigma)}}, \quad \hat{q}_k^{(\sigma)} = \ln \hat{Q}_k^{(\sigma)}. \tag{27}$$

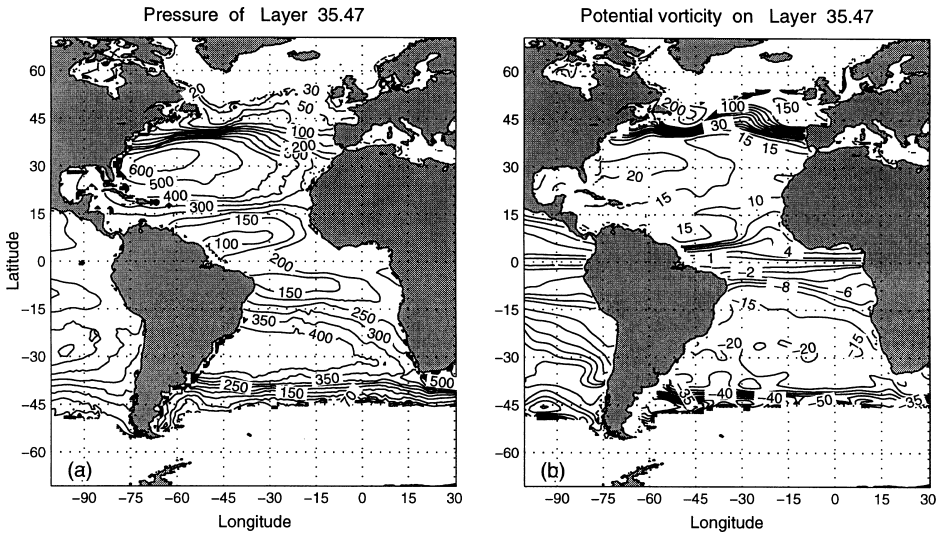

Fig. 4. Climatological ($\hat{p}$, $\hat{Q}$) data on σ_2 = 35.47 (kg/m^3) isopycnal surface: (a) pressure, $\hat{p}$ (unit: db), and (b) potential vorticity, $\hat{Q}$ (unit: 10^{-11} m^{-1}s^{-1}).

Having the climatological ($\hat{h}_k^{(\sigma)}$, $\hat{Q}_k^{(\sigma)}$) data (Fig. 4), it is easy to invert the absolute velocity on the potential-density surfaces. After checking the whole data set, we found the existence of the ***P***-spiral at all water columns of the Atlantic Ocean on $1° \times 1°$ grid. Earlier work (e.g., McCartney, 1982; Keffer, 1985; Talley, 1988) also shows the benefit of using potential vorticity in ocean circulation studies.

6.4 Parameter Λ

The spatial variability of the parameter Λ represents the spatial variability of the P-vector spirals. For illustration, we chose six locations (Fig. 5), A (54°W, 20°N), B (36°W, 28°N), C (20°W, 55°N), D (57°W, 40°N), E (18°W, 6°S), and F (30°W, 45°N), where the first three locations were studied extensively in the past (e.g., Schott and Stommel, 1978; Stommel and Schott, 1997). These six points represent the Antilles Current, North Atlantic Gyre, Norwegian Current, Gulf Stream, South Equatorial Current, Antarctic Circumpolar Current, respectively. We computed the parameter $\Lambda(\sigma_2)$ at each σ_2-level for the six locations (Fig. 6). The values of $\Lambda(\sigma_2)$ are usually small in the upper isopycnal layers, and become large in deeper isopycnal layers.

To quantitatively estimate the turning angle between the two consecutive isopycnal layers, we discretize (17) into

$$\Delta\phi = \Lambda. \tag{28}$$

For Λ = 0.2, the vertical turning angle is around 11°.

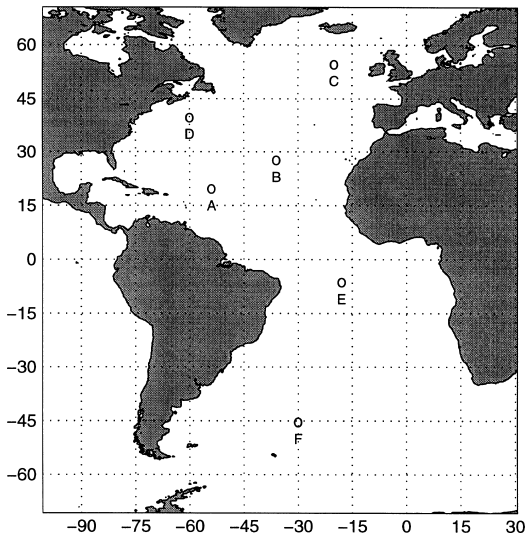

Fig. 5. Six locations chosen for illustration: the Antilles Current (A), North Atlantic Gyre (B), Norwegian Current (C), Gulf Stream (D), South Equatorial Current (E), Antarctic Circumpolar Current (F).

7. Zonally Integrated Latitudinal Transport

Following Wunsch and Grant (1982), we integrate the inverted velocity *v* zonally (Fig. 7) and study the flow in the meridional plane. The flow (Fig. 7) shows similar patterns as depicted in Wunsch and Grant (1982). The dominant features are poleward movement above about

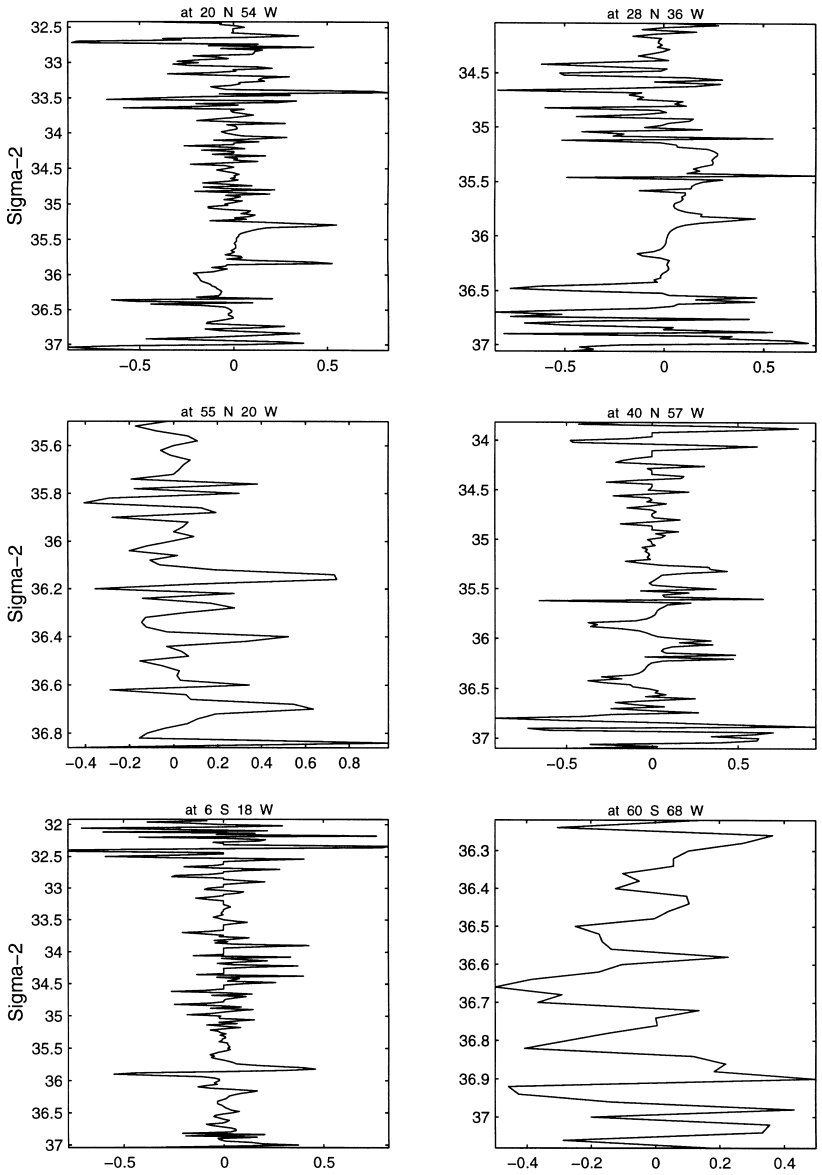

Fig. 6. Climatological P-vector spiral parameter (Λ) at several locations.

σ_0 = 27.76 with equatorward movement below that, in general accord with the conventional picture of what should happen. The maximum northward motion in the upper layer ($\sigma_0 \geq 27.76$) occurs at 35°N with a transport of 59.9 Sv (1 Sv = 10^6 m^3/s). Our model also shows the system changes from a net downwelling from the upper layers into the deep water poleward of 40°N, to a net upwelling through the water column equatorward of that latitude. This consists with earlier studies by Wunsch and Grant (1982).

8. Conclusions

(1) In this study, we prove that the conventional view on the validity of the inversion (existence of velocity spiral) is true only for a system with no μ-effect and no diapycnal velocity. For a system with either the μ-effect or the diapycnal velocity, the validity of the inversion is the existence of the ***P***-spiral.

(2) The ***P***-spiral occurs when the potential vorticity ($q^{(\sigma)}$) and its vertical gradient ($\partial q^{(\sigma)}/\partial z^{(\sigma)}$) are nonzero and independent. These spirals are featured by the rotation of

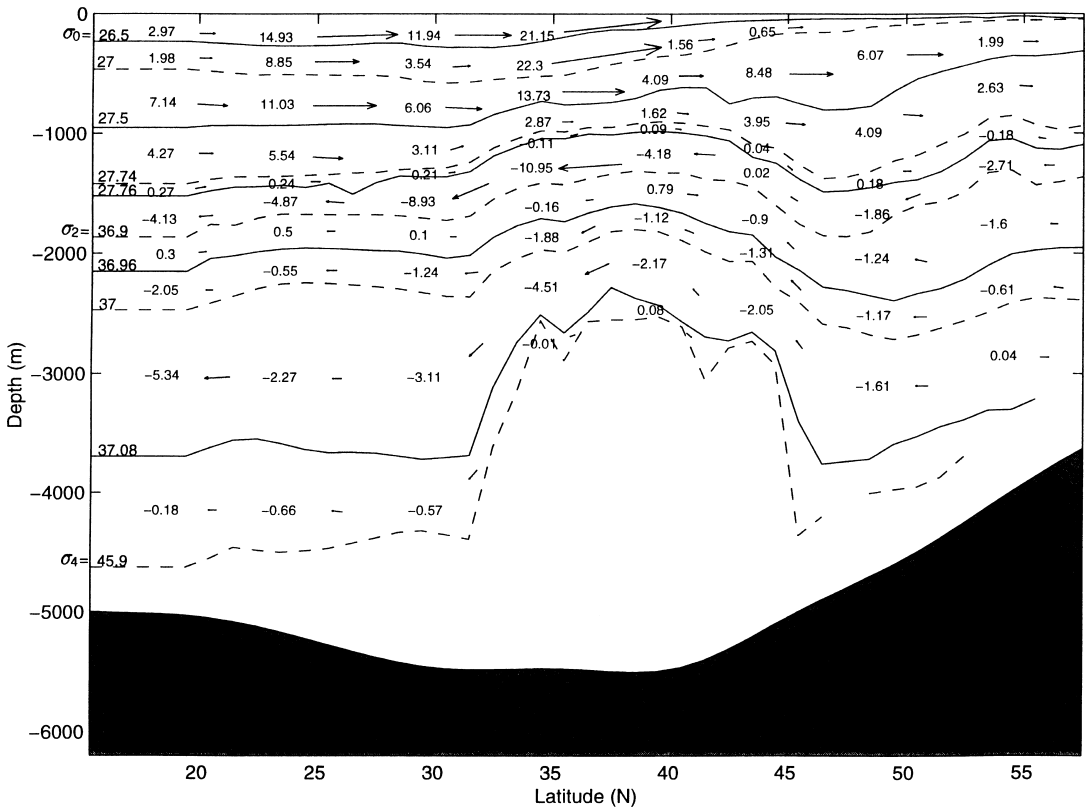

Fig. 7. Zonally integrated latitudinal transport (Sv) between two adjacent isopycnal levels inverted from NODC climatological mean *T*, *S* data. The size of the vector indicates the magnitude of the volume transport.

the unit vector, ***P***, on the isopycnal surface with potential density. Using the climatological *T*, *S* data, we found that the ***P***-spirals exist almost everywhere in the world oceans.

(3) Based on the potential vorticity conservation, we developed the ***P***-spiral method to invert the absolute geostrophic velocity on the potential-density surfaces. This method can invert the absolute velocity on the potential-density surfaces for a dynamical system including the μ-effect and the diapycnal velocity, and has great potential for investigating the general ocean circulations.

Acknowledgements

The author deeply thanks Rongfeng Li and Chenwu Fan for invaluable discussion and programming assistance and two anonymous reviewers for their critiques, which significantly improved this paper. This work was funded by the Office of Naval Research Naval Ocean Modeling and Prediction (NOMP) Program.

References

Behringer, D. W. (1979): On computing the absolute geostrophic velocity spiral. *J. Mar. Res.*, **37**, 459–470.

Behringer, D. W. and H. Stommel (1980): The beta spiral in the North Atlantic subtropical gyre. *Deep-Sea Res.*, **27A**, 225–238.

Chu, P. C. (1995): P-vector method for determining absolute velocity from hydrographic data. *Mar. Tech. Soc. J.*, **29**(3), 3–14.

Chu, P. C. and R. F. Li (2000): South China Sea isopycnal surface circulations. *J. Phys. Oceanogr*. (in press).

Chu, P. C., C. W. Fan and W. J. Cai (1998a): P-vector inverse method evaluated using the Modular Ocean Model (MOM). *J. Oceanogr.*, **54**, 185–198.

Chu, P. C., C. W. Fan, C. J. Lozano and J. Kerling (1998b): An airborne expandable bathythermograph (AXBT) survey of the South China Sea, May 1995. *J. Geophys. Res.*, **103**, 21637–21652.

Coats, D. A. (1981): An estimate of absolute geostrophic velocity from the density field in the northeastern Pacific Ocean. *J. Geophys. Res.*, **86**, 8031–8036.

Davis, R. (1978): On estimating velocity from hydrographic data. *J. Geophys. Res.*, **83**, 5507–5509.

Keffer, T. (1985): The ventilation of the world's oceans: maps of the potential vorticity field. *J. Phys. Oceanogr.*, **15**, 509–523.

Killworth, P. (1986): A Bernoulli inverse method for determining the ocean circulation. *J. Phys. Oceanogr.*, **16**, 2031–2051.

Levitus, S. and T. Boyer (1994): World Ocean Atlas, Vol. 4: Temperature. *NOAA Atlas NESDIS*, **4**, U.S. Gov. Printing Office, Washington, D.C., 117 pp.

Levitus, S., R. Burgett and T. Boyer (1994): World Ocean Atlas, Vol. 3: Salinity. *NOAA Atlas NESDIS*, **3**, U.S. Gov. Printing Office, Washington, D.C., 99 pp.

McCartney, M. S. (1982): The subtropical recirculation of Mode Waters. *J. Mar. Res.*, **40**(Suppl.), 427–464.

McDougall, T. J. (1988): Neutral-surface potential vorticity. *Prog. Oceanogr.*, **20**, 185–221.

McDougall, T. J. (1995): The influence of ocean mixing on the absolute velocity vector. *J. Phys. Oceanogr.*, **25**, 705–725.

Olbers, D. J., M. Wenzel and J. Willbrand (1985): The inference of North Atlantic circulation patterns from climatological hydrographic data. *Rev. Geophys.*, **23**, 313–356.

Schott, F. and H. Stommel (1978): Beta spirals and absolute velocities in different oceans. *Deep-Sea Res.*, **25**, 961–1010.

Stommel, H. and F. Schott (1977): The beta spiral and the determination of the absolute velocity field from hydrographic station data. *Deep-Sea Res.*, **24**, 325–329.

Talley, L. D. (1988): Potential vorticity distribution in the North Pacific. *J. Phys. Oceanogr.*, **18**, 89–106.

Wunsch, C. (1978): The general circulation of the North Atlantic west of 50°W determined from inverse method. *Rev. Geophys.*, **16**, 583–620.

Wunsch, C. and B. Grant (1982): Towards the general circulation of the North Atlantic Ocean. *Prog. Oceanogr.*, **11**, 1–59.